Articles

Phenylalanyl-tRNA Synthetase of *Escherichia coli* K10. Effects of Zinc(II) on Partial Reactions of Diadenosine 5′,5‴-P^1,P^4-Tetraphosphate Synthesis, Conformation, and Protein Aggregation†

Ottmar Goerlich and Eggehard Holler*

ABSTRACT: The synthesis of diadenosine 5′,5‴-P^1,P^4-tetraphosphate (Ap_4A) catalyzed by phenylalanyl-tRNA synthetase in the presence of Zn^{2+} involves the same partial reactions (synthesis of phenylalanyladenylate and transfer of the adenylate moiety to ATP) as occur in the absence of this metal ion. However, transfer is strongly stimulated while adenylate synthesis is depressed. Also inhibited are pyrophosphorolysis of phenylalanyladenylate and transfer of phenylalanine from the adenylate to cognate tRNA, because overall tRNA phenylalanylation is depressed [Mayaux, J.-F., & Blanquet, S. (1981) *Biochemistry 20*, 4647–4654], whereas binding of tRNA to the synthetase is not. At moderate concentrations of Zn^{2+}, and in the presence of 5 μM phenylalanine and 0.5 mM ATP, transfer of AMP is rate limiting, while at higher concentrations of Zn^{2+} synthesis of adenylate is rate determining. The Zn^{2+} concentration optimum for stimulation depends on the concentration of phenylalanine and ATP. The effects of Zn^{2+} are mediated through two classes of binding site(s) on the synthetase, the half-saturations of which are 1–4 and 20–30 μM Zn^{2+}, respectively. Binding of Zn^{2+} to the second class of site(s) causes inhibition of the synthetase, whereas binding to the first class is responsible for activation and inhibition, which may be caused by a conformational change. Evidence for the latter is the observed decrease in protein intrinsic fluorescence intensity and the decrease in fluorescence intensity of 6-(*p*-toluidinyl)naphthalene-2-sulfonate, which is used as a reporter group. The kinetics of the binding reaction show a saturation dependence on Zn^{2+}, also suggesting that a conformational change occurs. Binding of Zn^{2+} to the second class of site(s) is monitored by an increase in the fluorescence intensity, although this can be attributed to Zn^{2+}-promoted binding of 6-(*p*-toluidinyl)-naphthalene-2-sulfonate by the synthetase. A third type of Zn^{2+} binding site (half-saturation concentration > 50 μM Zn^{2+}) is involved in the aggregation of phenylalanyl-tRNA synthetase at 37 °C that is EDTA reversible. The substrates $tRNA^{Phe}$, MgATP, and phenylalanine are protective, and Mg^{2+} intensifies aggregation. Aggregation is considerably faster (more than 10-fold) at 37 °C than at room temperature and is not specific for that kind of protein, though the concentrations of Zn^{2+} that are effective can vary. The importance of aggregation is discussed in the light of the proposed regulatory role of zinc ions. Evidence obtained from steady-state kinetics of Ap_4A synthesis shows that a phenylalanine chelate of Zn^{2+} may be involved in stimulation. The rate-concentration dependence is biphasic with Michaelis–Menten constants of 30 μM and 0.9 mM. While the first value seems to reflect the dissociation constant of the synthetase–phenylalanine complex, the second value is compatible with chelation of Zn^{2+} by phenylalanine.

Phenylalanyl-tRNA synthetase catalyzes the phenylalanylation of tRNA involving partial reactions known as (1) activation of phenylalanine and (2) transfer of the phenylalanyl moiety to $tRNA^{Phe}$ (Baltzinger & Holler, 1981). The enzyme also catalyzes the transfer of activated AMP to ATP, synthesizing Ap_4A[1] (Goerlich et al., 1982). Catalysis of this type of reaction is a property of several of the members of the aminoacyl-tRNA synthetase family (Zamecnik et al., 1966; Plateau et al., 1981; Goerlich et al., 1982). Ap_4A has been proposed to be an important signal compound that might be involved in the regulation of cell growth (Rapaport & Zamecnik, 1976; Grummt, 1978). Zinc ions are powerful activators of Ap_4A synthesis by phenylalanyl-tRNA synthetase and a few other aminoacyl-tRNA synthetases and may function as additional regulators of Ap_4A synthesis (Plateau et al., 1981; Goerlich et al., 1982).

Blanquet and co-workers have demonstrated that the overall phenylalanylation of tRNA and the ATP–PP_i exchange reaction were inhibited by Zn^{2+} while stimulation of Ap_4A synthesis occurred (Mayaux & Blanquet, 1981; Plateau et al., 1981). We describe here the effects of Zn^{2+} on the partial reactions of the catalytic pathways. Evidence is presented that Zn^{2+} exerts its effects by binding to the synthetase and at the same time provoking conformational changes.

We have also studied the general tendency of Zn^{2+} to induce aggregation of proteins and conclude that concentrations of free Zn^{2+} which results in stimulation of Ap_4A synthesis may also cause aggregation of proteins.

Materials and Methods

Aminoacyl-tRNA synthetases specific for Ile, Lys, Phe, and Tyr were purified from *Escherichia coli* K10 according to modified procedures of Hanke et al. (1974). Synthetases specific for Arg (yeast) and Trp (beef pancreas) were gifts from Drs. Gangloff (Strasbourg) and Labouesse (Bordeaux), respectively. The preparations had exactly the same properties

† From the Institut für Biophysik und Physikalische Biochemie der Universität Regensburg, D-8400 Regensburg, Federal Republic of Germany. *Received June 3, 1983.* The work was generously supported by the Deutsche Forschungsgemeinschaft.

[1] Abbreviations: EDTA, (ethylenedinitrilo)tetraacetic acid; Tris, 2-amino-2-(hydroxymethyl)-1,3-propanediol; Ap_4A, diadenosine 5′,5‴-P^1,P^4-tetraphosphate; TNS, 6-(*p*-toluidinyl)naphthalene-2-sulfonate; DTE, dithioerythritol.

0006-2960/84/0423-0182$01.50/0

as described previously (Goerlich et al., 1982). Aldolase (rabbit muscle), catalase (beef liver), ferritin (equine spleen), and thyroglobulin (beef thyroid) were from Pharmacia (Uppsala), and alcohol dehydrogenase (yeast), bovine serum albumin, chymotrypsin, inorganic pyrophosphatase (yeast), lysozyme (hen's egg white), pyruvate kinase (rabbit muscle), ribonuclease A (beef pancreas), ATP, ADP, AMP, Ap_4A, phosphoenolpyruvate, $tRNA^{Phe}$ (1500 pmol of phenylalanine acceptance/A_{260} unit of tRNA) were from Boehringer (Mannheim). 2-Amino-2-(hydroxymethyl)-1,3-propanediol (Tris) was purchased from Serva (Heidelberg), 6-(*p*-toluidinyl)naphthalene-2-sulfonate (TNS) and glycerol were from Sigma (Munich), [^{3}H]ATP and [^{14}C]Phe were from Amersham (Braunschweig), poly(ethylenimine)-impregnated cellulose sheets (Polygram Cel 300 PEI/UV_{254}) were from Machery Nagel (Düren), and nitrocellulose filters BA 85 were from Schleicher & Schüll (Dassel). Tryptophan synthase β_2 subunit from *Escherichia coli* was a gift from Dr. Bartholmes (Regensburg). All other reagents were of the highest available purity from Merck (Darmstadt). Double quartz-distilled water was used. All glassware was carefully rinsed before use. Proteins and tRNA were extensively dialyzed against several changes of 50 mM Tris-HCl buffer, pH 7.5, containing 0.2 mM EDTA and 0.2 mM dithioerythritol (for measurements with Zn^{2+}, these last two reagents were omitted from the final buffer).

The standard assay for Ap_4A synthesis was carried out in standard buffer (20 mM Tris-HCl, pH 7.5, buffer containing 10 mM $MgCl_2$, 0.1 mM EDTA, and 0.2 mM dithioerythritol) as described (Goerlich et al., 1982). When Zn^{2+} was included in the mixture, EDTA and dithioerythritol were omitted. Reaction products were analyzed by poly(ethylenimine) thin-layer chromatography as described (Goerlich et al., 1982). Rate constants, k_{obsd}, were calculated from initial rates by dividing these numbers by the concentration of active sites in each experiment.

Fast reactions were followed after rapid mixing in a quench-flow apparatus as has been described (Baltzinger & Holler, 1982; Kern & Gangloff, 1981). Reactions were terminated by rapid mixing with 100 mM EDTA (pH 7.5), and products were analyzed either by the nitrocellulose filter assay (Goerlich et al., 1982) or by thin-layer chromatography.

In stopped-flow measurements, intensities either of protein-intrinsic fluorescence or of the fluorescence of TNS were followed as described (Baltzinger & Holler, 1982). Several records were collected for each set of experimental conditions, and the average time dependence was calculated by using a computer program that included two exponential functions. This was done in steps: first by fitting the slowest reaction to given parameters, the reaction amplitude, and k_{obsd} and then by employing the calculated time dependence as the base line for the fitting procedure to the fast reaction.

Association of Zn^{2+} with phenylalanyl-tRNA synthetase at equilibrium was measured in the presence of TNS in a Perkin-Elmer MPF 44 A spectrofluorometer at 25 °C as described (Kosakowski & Holler, 1973). Aggregation of proteins in the presence of Zn^{2+} was followed at 400 nm in a Zeiss DMR 10 spectrophotometer under temperature-controlled conditions.

Results

Overall Kinetics of Ap_4A Synthesis. The synthesis of Ap_4A was stimulated by Zn^{2+} ions (Plateau et al., 1981; Goerlich et al., 1982), and the results are summarized in Table I. Maximal stimulation was 22-fold, and half-maximal stimulation was obtained in the presence of 10 μM Zn^{2+} (Figure 1). Higher concentrations of Zn^{2+}, however, were inhibitory,

Table I: Ap_4A Synthesis Catalyzed by Phenylalanyl-tRNA Synthetase

experimental conditions[a]	Zn^{2+} (μM)	substrate varied		k_{cat} (s^{-1})	K_m (mM)
1.5 mM Phe		MgATP		0.26 ± 0.05[b]	50 ± 10[b]
1.5 mM Phe	60	MgATP		1.3 ± 0.1[b]	9 ± 1[b]
2.0 mM MgATP	60	Phe:	low	0.11 ± 0.01	0.03 ± 0.005
			high	0.47 ± 0.05	0.9 ± 0.2

[a] Standard assay for Ap_4A synthesis, 37 °C. [b] Goerlich et al. (1982).

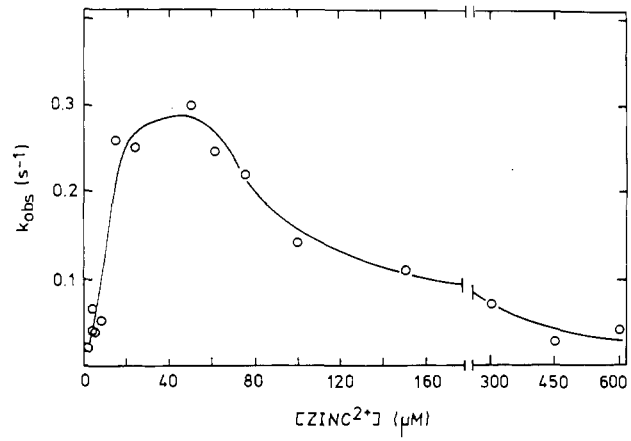

FIGURE 1: Overall rate constant for Ap_4A synthesis as a function of Zn^{2+} concentration. Conditions were as in the standard assay except that EDTA and dithioerythritol were omitted from the reaction mixture.

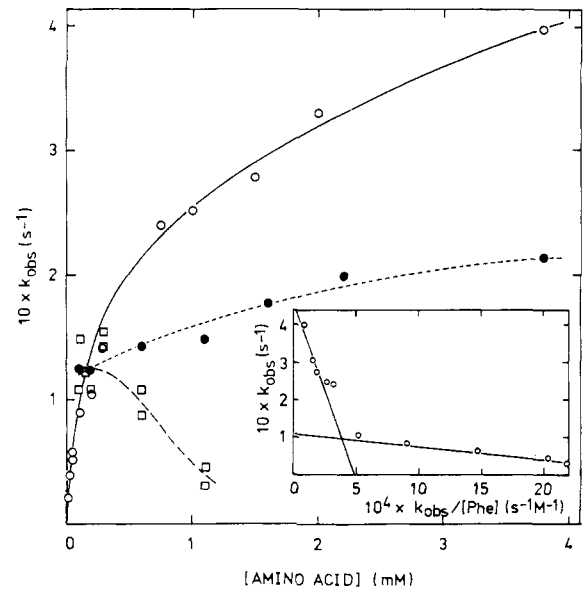

FIGURE 2: Overall rate constant of Ap_4A synthesis as a function of phenylalanine concentration. Effects of glycine and histidine. Conditions were those used in the standard assay except that solutions contained 60 μM Zn^{2+} and no EDTA and dithioerythritol. Total enzyme concentration was 0.4 μM. Symbols refer to varied concentrations of (○) phenylalanine, (●) glycine and 100 μM Phe, and (□) histidine and 100 μM Phe.

half-maximal inhibition being obtained in the presence of 100 μM Zn^{2+}. Stimulation could be resolved into a 5-fold decrease of the K_m(MgATP) and a 5-fold increase in k_{cat} when the concentration of Zn^{2+} was fixed at 60 μM and that of phenylalanine at 1.5 mM (Goerlich et al., 1982). When phenylalanine was the varied substrate (2 mM MgATP), the concentration dependence of the rate constant, k_{obsd}, was biphasic with k_{cat} and K_m(Phe) of 0.1 s^{-1}/30 μM at low and 0.47

s^{-1}/0.9 mM at high phenylalanine concentrations, respectively (Figure 2). When Zn^{2+} was absent from the reaction mixture, the concentration dependence closely followed the stoichiometric titration of phenylalanyl-tRNA synthetase as has been reported (Goerlich et al., 1982). This indicated K_m(Phe) values below the concentration of the enzyme and considerably below K_m(Phe) values reported here. Values could not be determined because at the low concentrations of enzyme required, synthesis of Ap_4A was not detectable.

Control experiments employing a low (100 μM) concentration of Phe and varying concentrations of Gly revealed that the noncognate amino acid also stimulated Ap_4A synthesis (Figure 2). In the absence of Phe and in the presence of 2 mM Gly, Ap_4A synthesis was not observed. Histidine, on the contrary, was inhibitory (Figure 2), probably due to chelation of Zn^{2+} (Hallman et al., 1971).

Synthesis of Phenylalanyladenylate. The rate constant for the synthesis of phenylalanyladenylate enzyme complex in the absence of Zn^{2+} ions was k_{obsd} = 6.4 s^{-1} (25 °C) as measured in a quench-flow apparatus after mixing (final concentrations) 5 μM [^{14}C]Phe (200 μCi/μmol), 0.5 mM MgATP, 0.22 μM phenylalanyl-tRNA synthetase, and 10 μg/mL inorganic pyrophosphatase in standard buffer (containing 0.1 mM EDTA and 0.2 mM DTE). In the reaction, 1.6 mol of [^{14}C]phenylalanyladenylate was formed per mol of synthetase. Kinetics were strictly first order (not shown), suggesting that both active centers (Bartmann et al., 1975) reacted independently. In the presence of 60 μM Zn^{2+} in both drive syringes (buffer without EDTA and DTE), adenylate synthesis was not detected within the time (0.4 s) of observation. This suggested that the presence of Zn^{2+} led to suppression of the reaction rate by at least a factor of 100. The dependence on Zn^{2+} concentration was measured by the fluorometric stopped-flow technique described previously (Baltzinger & Holler, 1982, and references therein). The standard reaction in the absence of Zn^{2+} (5 μM TNS but otherwise the same conditions as in the quench-flow experiment) was strictly single exponential with k_{obsd} = 3.3 s^{-1}. Part of the discrepancy with respect to the value from the quench-flow experiment reflects competitive inhibition by TNS as has been discussed (Pimmer & Holler, 1979).

With varying concentrations of Zn^{2+} in both drive syringes, the value of k_{obsd} decreased hyperbolically with an inhibition constant K_i = 3 μM (not shown). For [Zn^{2+}] > 35 μM, reaction amplitudes were unmeasurably small, and k_{obsd} could not be determined. The value of K_i (3 μM) was used to calculate $k_{obsd} = k_{obsd}(0)(1 - [Zn^{2+}]/(K_i + [Zn^{2+}])) = 0.3$ s^{-1} for [Zn^{2+}] = 60 μM and $k_{obsd}(0)$ = 6.4 s^{-1} from the quench-flow experiment. As mentioned, however, k_{obsd} was smaller than 0.064 s^{-1} obtained by quench-flow measurements. We take the discrepancy as evidence for further inhibition at high concentrations of the metal ion.

Synthesis of Ap_4A from Phenylalanyladenylate and ATP. Phenylalanyl[^{3}H]adenylate synthetase complex that had been prepared in situ in the absence of Zn^{2+} was mixed in the quench-flow apparatus with 10 mM (final) MgATP and 60 μM (final) Zn^{2+}. The preformed adenylate (1.3 mol/mol of enzyme, by nitrocellulose filter assay) was consumed in a single exponential time-dependent reaction with k_{obsd} = 0.9 s^{-1} (Figure 3, upper panel). Controls in the absence or presence of small amounts of MgATP (50 μM) indicated that adenylate consumption in the presence of Zn^{2+} was not due to a metal ion induced destabilization of the enzyme–adenylate complex.

Reaction products were analyzed by PEI thin-layer chromatography in the presence of chymotrypsin (Figure 3, lower panel) (Goerlich et al., 1982). Note that adenylate is hydrolyzed under these conditions to [^{3}H]AMP. Kinetics were single exponential, and k_{obsd} values were 0.7 s^{-1} for [^{3}H]AMP and 0.9 s^{-1} for [^{3}H]Ap_4A. Adenylate was quantitatively converted to Ap_4A (Figure 3, lower panel).

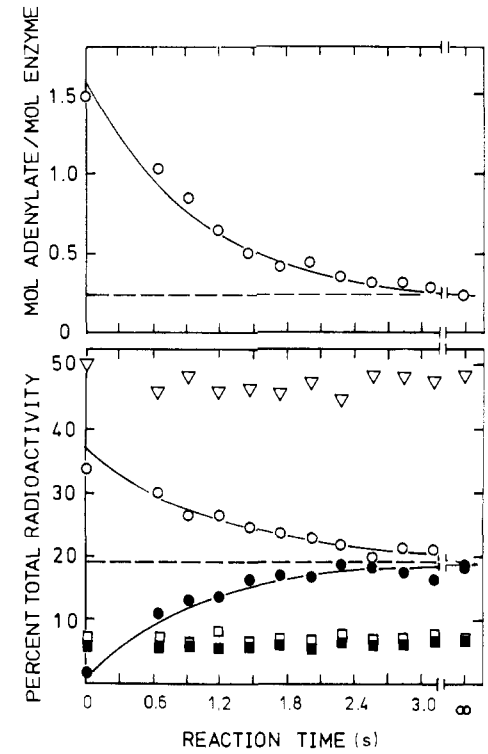

FIGURE 3: Partial reaction of Ap_4A synthesis from phenylalanyladenylate–enzyme complex. Radioactively labeled adenylate enzyme that had been prepared in situ was mixed in a quench-flow apparatus with a large amount of unlabeled MgATP and Zn^{2+}. One syringe contained 5.7 μM [^{3}H]ATP (9.4 mCi/μmol), 20 μM Phe, 0.88 μM phenylalanyl-tRNA synthetase, 20 μg/mL inorganic pyrophosphatase, standard buffer (without EDTA and dithioerythritol), and an ATP-regenerating system that consisted of 5 μg/mL pyruvate kinase and 200 μM phosphoenolpyruvate. The other syringe contained 20 mM MgATP, standard buffer (without EDTA and dithioerythritol), and 120 μM $ZnCl_2$. Reaction temperature was 37 °C. At varying times the reaction was terminated by the addition of 100 μM EDTA from a third syringe. (Upper panel) Unreacted enzyme–adenylate complex was measured by the nitrocellulose filter assay. A constant level of 0.3 mol of adenylate/mol of enzyme was unreactive, even at prolonged incubation times. This radioactivity was probably due to an unrecognized side reaction and was subtracted as background. (Lower panel) Separation and analysis by PEI thin-layer chromatography. [^{3}H]Ap_4A (●), [^{3}H]AMP (in part as hydrolyzed adenylate) (○), [^{3}H]ATP (▽), [^{3}H]ADP (□), and [^{3}H]Ap_3A (■). Percent radioactivity was calculated relative to total radioactivity in each sample. Reaction amplitudes were equal to 1.1 mol of adenylate and Ap_4A, respectively, per mol of enzyme. Solid curves were computed on the basis of single exponential time dependences, the rate constants given in the text, and the levels of reactants at equilibrium (---). Note that the remaining high level of AMP originates from hydrolysis of adenylate in the storage syringe prior to Ap_4A synthesis (blank value).

Steady-State Concentration of Phenylalanyladenylate–Enzyme Complex. The concentration of the intermediate, phenylalanyladenylate, was measured by the nitrocellulose filter assay after termination of the reaction (5 min at 25 °C) by mixing with 50 mM EDTA (Figure 4). It was not known whether the time for approaching steady state was dependent on the point of addition of Zn^{2+}. Therefore, we performed two sets of experiments. In one, the metal ion was added to the reagent solutions before and, in the other, it was added after the initiation of Ap_4A synthesis. In control experiments it was verified that steady state was sustained at least 3–10 min after mixing of reactants.

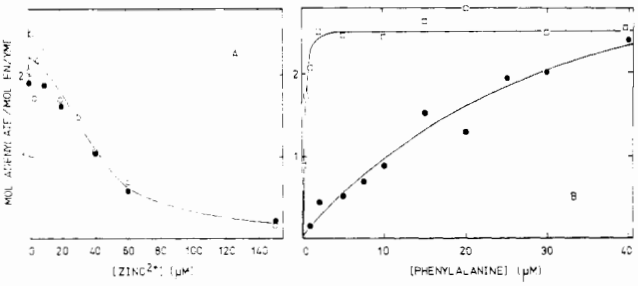

FIGURE 4: Steady-state concentration of phenylalanyladenylate–enzyme complex during Ap_4A synthesis. The reaction mixture in (A) contained 5 μM [^{14}C]Phe (200 μCi/μmol), 0.5 mM MgATP, 0.34 μM phenylalanyl-tRNA synthetase, 10 μg/mL inorganic pyrophosphatase, 20 mM Tris-HCl (pH 7.5), and 10 mM $MgCl_2$. Incubation temperature was 25 °C. $ZnCl_2$ was added before (●) or after (○) the enzyme. (B) The concentration of [^{14}C]Phe (50–200 μCi/μmol) was varied. Reaction mixtures contained 2 mM MgATP, 0.2 μM phenylalanyl-tRNA synthetase, 10 μg/mL inorganic pyrophosphatase, and standard buffer, and were incubated at 37 °C (□). In the presence of 60 μM $ZnCl_2$ (●), EDTA and dithioerythritol were omitted from the reaction mixture.

The order of addition of Zn^{2+} and initiation of Ap_4A synthesis did not affect the results (Figure 4). The amount of adenylate enzyme complex decreased in a sigmoidal fashion as a function of Zn^{2+} concentration. This is to be expected if the rates of the partial reactions change in opposite directions. Synthesis of adenylate is faster than its conversion to Ap_4A at 0–35 μM Zn^{2+} and slower at higher concentrations of Zn^{2+}. Note that adenylate synthesis is irreversible when inorganic pyrophosphatase is not limiting, ruling out the possibility that the levels of adenylate measured reflect the Zn^{2+} dependence of the reaction equilibria.

The steady-state concentration of adenylate enzyme complex is a function of phenylalanine concentration (Figure 4B). In the absence of Zn^{2+}, a maximum steady-state concentration is obtained after saturation of both active sites with adenylate at the point where the amount of Phe equals that of active sites, due to the rapid synthesis of adenylate and the irreversibility of the reaction. In the presence of 60 μM Zn^{2+}, conversion of adenylate is faster than its synthesis, and consequently, the steady-state concentration is low. As long as synthesis is rate limiting, the increase of the steady-state concentration of adenylate will reflect the binding curve for Phe. The concentration at half-maximum, 15 μM Phe, is in agreement with the value for K_{diss}(Phe) of 19–30 μM obtained by Bartmann et al. (1975). This finding rules out that the biphasic steady-state kinetics of Ap_4A synthesis (Figure 2) are due to nonequivalent active sites.

Pyrophosphorolysis of Phenylalanyladenylate. Enzyme–[^{14}C]phenylalanyladenylate complex synthesized in situ [1.8 mol of adenylate/mol enzyme in the presence of 100 μM ATP, 4 μM [^{14}C]Phe (513 μCi/μmol), 0.44 μM synthetase, 0.5 μg/mL pyrophosphatase, and standard buffer, incubated 5–10 min at 25 °C] was mixed with a solution of 30 μM PP_i (final) in the presence or absence of 60 μM Zn^{2+} in the quench-flow apparatus (25 °C). After termination of the reaction with 50 mM EDTA (final), adenylate–enzyme complex was determined by the nitrocellulose filter assay. Kinetics were single exponential with rate constants of 8.9 s^{-1} in the absence and 1.6 s^{-1} in the presence of Zn^{2+}.

Interaction of Zn^{2+} with Phenylalanyl-tRNA Synthetase. The interaction of Zn^{2+} with the synthetase was measured at equilibrium and by fast kinetic techniques that followed the fluorescence intensity of reversibly enzyme-bound TNS. Titration of the synthetase with Zn^{2+} led to a small decrease at 2 μM Zn^{2+} and to a subsequent increase in fluorescence intensity (Figure 5A, inset). A biphasic dependence was also obtained in the presence of 10 mM $MgCl_2$, except that the decrease in fluorescence intensity affected by Zn^{2+} was considerably larger. Mg^{2+} is known to effect an increase in fluorescence intensity (Pimmer & Holler, 1979). No change

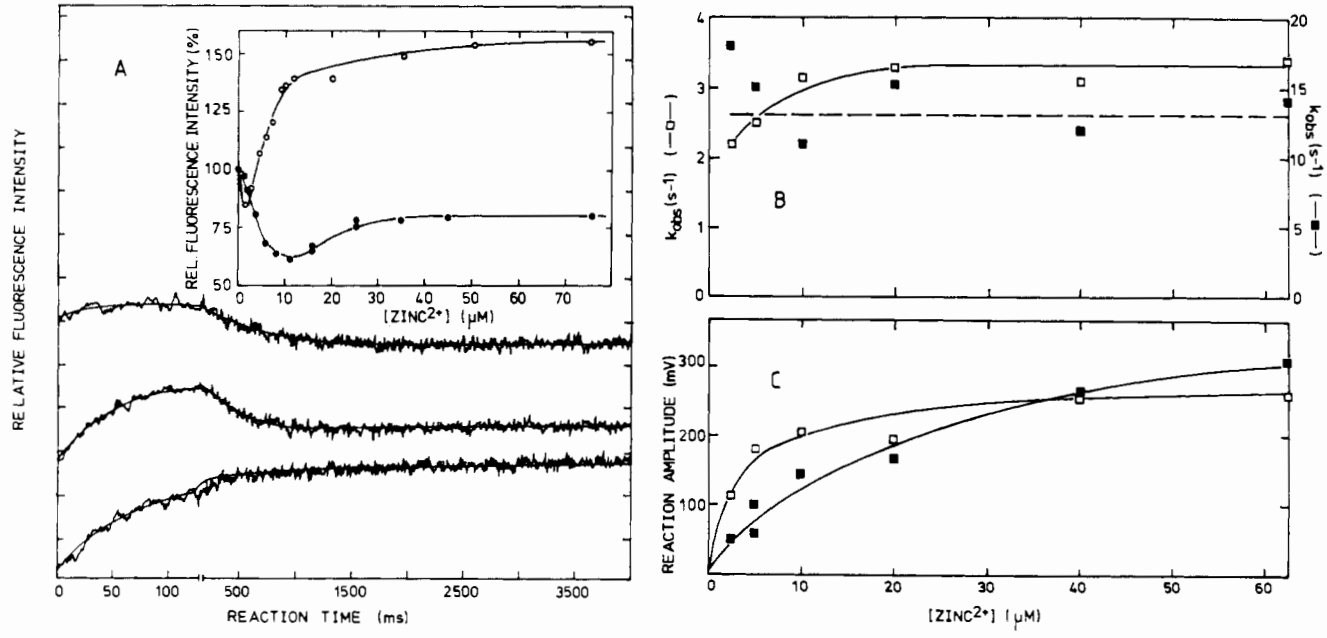

FIGURE 5: Association of phenylalanyl-tRNA synthetase and Zn^{2+} in the presence of the fluorescent reporter TNS. Concentrations were 0.15–0.3 μM phenylalanyl-tRNA synthetase, 5 μM TNS, and 20 mM Tris-HCl (pH 7.5 and 25 °C). (Panel A, inset) the relative fluorescence intensity (excitation 320 nm, emission 450 nm) at equilibrium in the absence (○) and in the presence (●) of 10 mM $MgCl_2$. (Panel A) Time dependence of the fluorescence intensity after mixing of enzyme and 5 μM $ZnCl_2$ (upper trace), 60 μM $ZnCl_2$ (middle trace), or 60 μM $ZnCl_2$ plus 4 mM Phe (lower trace), respectively, in a stopped-flow apparatus. One scale unit refers to 100 mM. (Panel B) Rate constants that gave the best fit of two superimposed time dependences to the measured traces in panel A. Symbols refer to intensity increase (■) and decrease (□), respectively, in panel A including the inset. (Panel C) Reaction amplitudes of the traces in panel A, absolute values. Symbols are as in panel B.

was seen in the absence of synthetase.

The different phases indicated at least two types of binding sites for Zn^{2+}, a high-affinity class (2–4 μM at half-maximum intensity change) and a low-affinity class (7–20 μM, depending on whether $MgCl_2$ was present). The first of the reactions was eliminated in the presence of 10 mM Phe. The intensity changes were probably caused by different TNS molecules, one of them occupying the Phe-specific binding site as had been noted (Kosakowski & Holler, 1973).

Kinetics were followed by the stopped-flow technique after mixing of enzyme/TNS with Zn^{2+} solutions (Figure 5). Time dependences were biphasic (Figure 5A). Solid curves in the figure were computed on the basis of the best fit to the experimental data by two exponentials. Corresponding rate constants and reaction amplitudes are shown in Figure 5B,C. The concentration dependence of the amplitudes was similar to that in the titration experiments (Figure 5A, inset). The reaction with the intensity increase was fast compared with the reaction that was characterized by an intensity decrease (Zn^{2+} concentration of 2–3 μM at half-maximum). The rate constants for the fast reaction became highly inaccurate at low Zn^{2+} concentrations because of very low amplitudes. The presence of 4 mM Phe eliminated the slow reaction in agreement with the results of the titration experiment.

The order of mixing was reversed in a control experiment by adding a mixture of synthetase and Zn^{2+} (40 μM) to a mixture of TNS (final 5 μM) and Zn^{2+} (40 μM). The observed intensity increase was biphasic (k_1 = 16 s^{-1} and k_2 > 100 s^{-1}). Mixing of enzyme and TNS only gave rise to a single reaction with k > 100 s^{-1} [see also Pimmer & Holler (1979)]. The other, slow reaction (k_1 = 16 s^{-1}) was the result of the presence of Zn^{2+} and was of the same kind as observed when enzyme/TNS and Zn^{2+}/TNS solutions were mixed. This reaction was not abolished by the presence of Phe and must, therefore, involve a binding site for TNS other than the Phe-specific binding pocket of the synthetase (Baltzinger & Holler, 1981). The fast reaction in Figure 5A is thus likely to be the association of TNS to a site on the enzyme that has been exposed as the result of a much faster enzyme–Zn^{2+} complexation via the low-affinity site(s).

Kinetics were also measured by means of the enzyme-intrinsic tryptophan fluorescence after mixing solutions of synthetase and Zn^{2+} (60 mM final). The observed intensity decrease (about 3% at equilibrium) followed a rate constant (3.3 s^{-1}) similar to that of the slow intensity decrease in the case of the TNS fluorescence (Figure 5B). As in this case, the reaction was not seen in the presence of 2 mM Phe. Together with the finding that the rate constant leveled off with increasing concentrations of Zn^{2+}, the results demonstrate that complexation of Zn^{2+} with the high-affinity sites induced a conformational change in the synthetase.

Zinc Salt Induced Protein Aggregation. Because of its strong chelating properties, Zn^{2+} had to be considered as a general denaturant, particularly by stimulating protein aggregation. If Zn^{2+} was physiologically significant, aggregation should not be observed for any protein within the range of metal ion concentrations required for stimulation. In the presence of 150 μM or higher Zn^{2+}, where only partial stimulation of Ap_4A synthesis was observed (Figure 1), aggregation was discovered by absorbance measurement (400 nm, 37 °C) in the absence of substrates (Figure 6A). Time dependence was sigmoidal with a short lag phase followed by a single exponential absorbance increase. EDTA (1 mM) reversed aggregation completely and substrates MgATP (6.5 mM) and Phe (6.5 mM) partially. In the case where aggregation had been reversed by EDTA, tRNA aminoacylation activity was 70% of its original value.

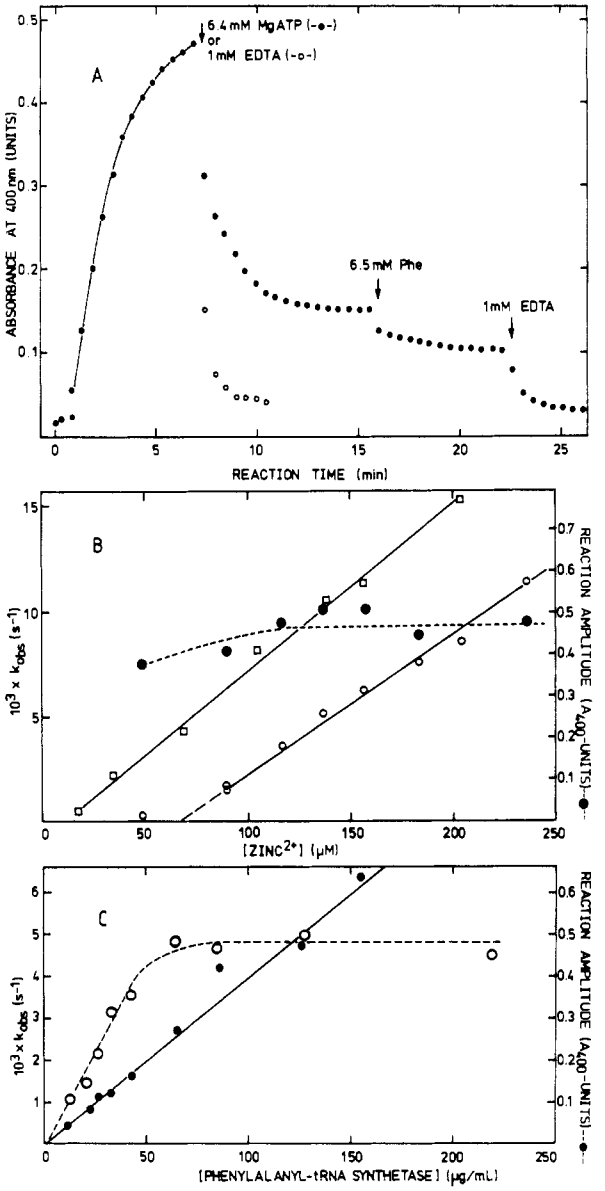

FIGURE 6: Aggregation of phenylalanyl-tRNA synthetase induced by $ZnCl_2$. Concentrations were 0.22 μM phenylalanyl-tRNA synthetase, 20 mM Tris-HCl, and, if not indicated otherwise, 10 mM $MgCl_2$. Reaction temperature was 37 °C. Turbidity was measured as absorbance at 400 nm in a spectrophotometer. Reaction amplitudes refer to the equilibrium level of light absorbance. (Panel A) Kinetics of aggregation. The solid curve is computed for a single exponential time dependence; values for k_{obsd} are shown in subsequent figures. Arrows indicate the addition of protective agents to the reaction mixture. (Panel B) Values of k_{obsd} as a function of $ZnCl_2$ concentration: (○) phenylalanyl-tRNA synthetase, (□) isoleucyl-tRNA synthetase, and (●) the reaction amplitude for phenylalanyl-tRNA synthetase. (Panel C) Values of k_{obsd} (○) and the reaction amplitude (●) as functions of the concentration of phenylalanyl-tRNA synthetase.

Over 80% of the absorbance increase followed the observed single exponential time dependence. Rate constants were measured as a function of concentration of Zn^{2+} (Figure 6B) and of phenylalanyl-tRNA synthetase (Figure 6C). The minimum requirement for zinc ions was about 70 μM, from whereon k_{obsd} increased linearly. The protein dependence was linear up to 50 μg/mL synthetase, and then k_{obsd} remained constant. Reaction amplitudes did not show a significant dependence on the concentration of zinc ions and were a linear function of the protein concentration. The aggregation equilibrium was slightly endothermic (50% increase in ab-

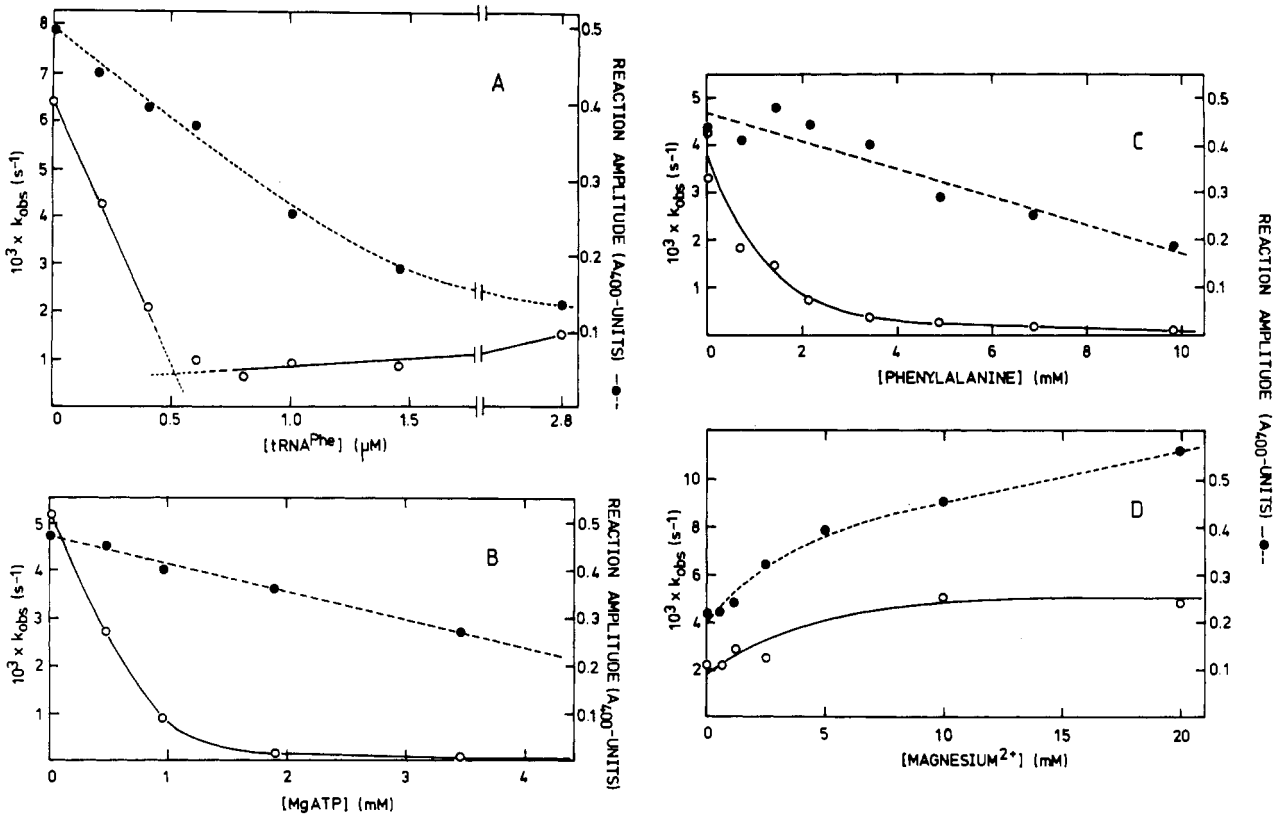

FIGURE 7: Protection against Zn^{2+}-induced aggregation of phenylalanyl-tRNA synthetase. Conditions were as described for Figure 6, with constant 155 μM $ZnCl_2$. The symbol ● refers to the reaction amplitude. (Panel A) Protection by $tRNA^{Phe}$. (Panel B) Protection by MgATP. (Panel C) Protection by phenylalanine. (Panel D) Protection by $MgCl_2$. In this case, the buffer did not contain extra $MgCl_2$.

sorbance between 25 and 35 °C). Rate constants were strongly temperature dependent (5-fold increase between 25 and 35 °C, Arrhenius energy of 35 kcal/mol). Because of this complexity, a kinetic model was not attempted at present.

The ability of other metal ions to induce aggregation was investigated for Ca^{2+}, Mn^{2+}, Co^{2+}, Ni^{2+}, Cu^{2+}, and Cd^{2+} (20 mM Tris-HCl, pH 7.5, 10 mM $MgCl_2$, 155 μM metal ion, and 0.2 μM phenylalanyl-tRNA synthetase at 37 °C). Only Cd^{2+} and Cu^{2+} were effective, though at lower rates than Zn^{2+}.

The potential for aggregation of other proteins was investigated by using a random selection of various proteins. Lysyl-tRNA synthetase (*E. coli*), pyruvate kinase, and tryptophan synthase β_2 subunit (*E. coli*) were found to aggregate rapidly (k_{obsd} = 4–12 × 10^{-3} s^{-1}) in the presence of 7–10 μM Zn^{2+}, while aggregation of arginyl-tRNA synthetase (yeast), isoleucyl-tRNA synthetase (*E. coli*), tryptophanyl-tRNA synthetase (beef), tyrosyl-tRNA synthetase (*E. coli*), aldolase (rabbit), alcohol dehydrogenase (yeast), and catalase (beef) required 50–150 μM $ZnCl_2$. However, these concentrations were insufficient in the case of bovine serum albumin, lysozyme (hen), ribonuclease (beef pancreas), and thyroglobulin (beef). From these and other results we conclude that Zn^{2+} may stimulate aggregation of proteins in a nonspecific manner at metal ion concentrations as low as 7 μM, which is within the range observed for stimulation of Ap_4A synthesis.

It can be argued that proteins will be protected by binding their substrates. Protection experiments were carried out with phenylalanyl-tRNA synthetase and with aldolase (Figure 7 and Table II). Protection by $tRNA^{Phe}$ (Figure 7A) followed the stoichiometry of two molecules of $tRNA^{Phe}$ per molecule of phenylalanyl-tRNA synthetase in agreement with the number of binding sites on that enzyme (Bartmann et al., 1975). Interestingly, the finding ruled out the possibility that tRNA phenylalanylation was inhibited by Zn^{2+}, preventing

Table II: Protection against Aggregation of Phenylalanyl-tRNA Synthetase[a] or Aldolase[b]

protector	concn (mM)	$10^3 k_{obsd}$ (s^{-1})[c] phenylalanyl-tRNA synthetase[d]	aldolase[e]
none		7.9	3.4
ATP, Mg^{2+}[f]	2	0.5	0.43
ADP, Mg^{2+}	2	0.4	0.60
AMP, Mg^{2+}	2	17.6	3.1
dATP, Mg^{2+}	2	0.2	ND[g]
dAMP, Mg^{2+}	2	1.8	ND
GTP, Mg^{2+}	2	0.4	ND
cAMP, Mg^{2+}	2	9	ND
Ap_4A, Mg^{2+}	2	6	3.2
Phe	2	1.4	1.9
Gly	2	0.4	1.2
$tRNA^{Phe}$	0.001	0.9[h]	ND
	0.005	ND	3.1

[a] 20 mM Tris-HCl, pH 7.5, 155 μM $ZnCl_2$, 10 mM $MgCl_2$ at 37 °C. [b] Same as footnote *a* but 50 μM $ZnCl_2$. [c] Calculated from the single exponential A_{400} increase. [d] 0.2 μM. [e] 1.8 μM. [f] Equivalent concentrations of nucleotide and $MgCl_2$. [g] ND = not determined. [h] Conditions as in Figure 7A.

$tRNA^{Phe}$–synthetase complex formation. Other protectors may be considered as nonspecific because of their protective effects on aldolase, for which they were not substrates (Table II), and because of their ability to form chelates (Table IV). Other observations in Table II and Figure 7 are interesting. AMP·Mg but not dAMP·Mg promoted aggregation of phenylalanyl-tRNA synthetase, but not that of aldolase. The finding is not understood, at present. Mg^{2+} also supported aggregation by Zn^{2+} (Figure 7D). The concentration dependence is reminiscent of the known Mg^{2+} binding isotherm for that enzyme (Pimmer & Holler, 1979) and suggests that stimulation could be the result of direct association between

Table III: Concentration Dependences of Zn^{2+} Effects[a]

effect	reaction conditions	$[Zn^{2+}]_{0.5}$ (μM)[b] observed	corrected[c]
increase in fluorescence intensity	5 μM TNS	~7[d]	~7
titration	5 μM TNS + 10 mM $MgCl_2$	20	20
	5 μM TNS + 10 mM $MgCl_2$ + 10 mM Phe	>50	>7
amplitude[e]	5 μM TNS + 10 mM $MgCl_2$	20-30	20-30
decrease in fluorescence intensity	5 μM TNS	<2	<2
titration	5 μM TNS + 10 mM $MgCl_2$	4	4
amplitude[f]	5 μM TNS + 10 mM $MgCl_2$	2-3	2-3
equilibrium dialysis or protein fluorescence, titration[i]	150 mM KCl + 7 mM $MgCl_2$	1.3-1.7	ND
adenylate synthesis, inhibition	0.5 mM MgATP + 5 μM Phe + 5 μM TNS + 10 mM $MgCl_2$	3	2.4
steady-state concentration adenylate	0.5 mM MgATP + 5 μM Phe + 10 mM $MgCl_2$	40	30
tRNA phenylalanylation,[i] inhibition	2.5 μM $tRNA^{Phe}$ + 30-35 μM Phe + 2 mM ATP + 7 mM $MgCl_2$ + 150 mM KCl	5	ND
Ap_4A synthesis, 37 °C			
stimulation	1.5 mM Phe + 2 mM MgATP + 10 mM $MgCl_2$	10	3
inhibition	same	100	30
stimulation[g]	2 mM Phe + 2 mM MgATP + 5 mM $MgCl_2$ + 150 mM KCl	30	ND[h]

[a] 20 mM Tris-HCl, pH 7.5, 25 °C, if not mentioned otherwise. [b] Concentration of $ZnCl_2$ at half-maximal effect. [c] See Appendix. [d] This class of sites appears to be inhomogeneous. [e] The amplitude of the fast intensity increase in Figure 6C. [f] The amplitude of the slow intensity decrease in Figure 6C. [g] Plateau et al. (1981). [h] ND = not determined. [i] Mayaux & Blanquet (1981).

Mg^{2+} and the synthetase. A surprising observation is that Ap_4A, although it chelates with Zn^{2+} (unpublished results), affords little protection.

With regard to shape and size of the aggregates, light absorbance was measured as a function of wavelength (150 μM Zn^{2+} and 0.4 μM phenylalanyl-tRNA synthetase). Values of ln (absorbance) plotted vs. ln (wavelength) followed a line with the slope of 2.3. The value is compatible with aggregates that are large in comparison to wavelengths (Gaskin et al., 1974; Berne, 1974). Electron micrographs (not shown) revealed filaments, sheets, and, in the case of isoleucyl-tRNA synthetase, piles of spherical structures. Similar observations have been reported for aggregation of tubulin in the presence of Zn^{2+} (Eagle et al., 1983). All these results confirm that aggregation is not protein specific.

Discussion

Zinc ions affect phenylalanyl-tRNA synthetase in various ways (Table III). (1) Activities of phenylalanyladenylate synthesis and of tRNA phenylalanylation (Mayaux & Blanquet, 1981) are suppressed, while a novel activity, synthesis of Ap_4A, is stimulated (Table III). (2) Of the partial reactions catalyzed by the enzyme, synthesis of phenylalanyladenylate is inhibited while its conversion by reaction with ATP to Ap_4A is stimulated. (3) Superposition of the effects leads to a substrate-dependent Zn^{2+} concentration optimum for Ap_4A synthesizing activity. (4) For moderate concentrations of Phe (5 μM) and MgATP (0.5 mM), the conversion is rate limiting at suboptimal and synthesis of adenylate at above optimal concentrations of Zn^{2+}. (5) After correction for chelation (Appendix), inhibition of tRNA phenylalanylation and adenylate synthesis and stimulation of adenylate conversion into Ap_4A seem to involve a single class of Zn^{2+} binding site(s) on the enzyme. Inhibition is enhanced by a second class of site(s) with lower affinity. (6) Association of Zn^{2+} with the "high-affinity sites" is followed by a fast conformational change. (7) Additional binding at higher concentrations of Zn^{2+} promotes reversible aggregation of the synthetase. (8) Substrates and EDTA protect against aggregation.

Kinetic Mechanism. Ap_4A synthesis follows a two-step path, first, activation of AMP and, second, condensation of the activated AMP with ATP and release of the amino acid (Zamecnik et al., 1966; Goerlich et al., 1982). We demonstrate here that the same pathway occurs in the presence of Zn^{2+} where it is the second partial reaction that is stimulated. Adenylate conversion and pyrophosphorolysis have been considered analogous (Zamecnik et al., 1966). However, pyrophosphorolysis is inhibited while conversion into Ap_4A is stimulated. This need not be a contradiction if, in the presence of Zn^{2+}, the rates of these reactions ultimately become identical.

Rate-Limiting Reaction. Whether conversion or synthesis of adenylate is rate limiting for the overall synthesis of Ap_4A will depend, in part, on the concentration of Zn^{2+} (Figure 4A), of Phe (Figure 4B), and of MgATP (not shown). The relative levels of Phe and MgATP will determine the optimal concentration of Zn^{2+} (Figure 1).

Rate limitation by adenylate synthesis is manifested as follows. (1) Rate constants for the overall synthesis of Ap_4A reflect the dissociation constant of the enzyme–Phe complex, if phenylalanine is the varied substrate. This is the case for the low concentration K_m(Phe) (30 μM; Figure 2) [K_{diss} = 19–30 μM (Bartmann et al., 1975)]. (2) Under the condition in Figure 5B, the steady-state concentration of adenylate in the range 0–45 μM Phe is mainly a function of the rate of adenylate synthesis. The concentration of Phe, 15 μM, at half-maximum adenylate compares with 19–30 μM of the dissociation constant of the enzyme–Phe complex. (3) Conditions of tRNA phenylalanylation in the presence of Zn^{2+} [2 mM ATP, 35 μM Phe, 7 mM $MgCl_2$, and 0–10 μM $ZnCl_2$ (Mayaux & Blanquet, 1981)] were such that adenylate synthesis was not rate limiting. The observed inhibition by Zn^{2+} must be involved in the Phe-transfer reaction. We have shown here by protection studies that binding of $tRNA^{Phe}$ to the synthetase is not abolished in the presence of Zn^{2+}.

High- and Low-Affinity Binding Sites for Zn^{2+}. The various effects of Zn^{2+} are displayed within characteristic concentration ranges of the metal ion. These are summarized in terms of concentrations at half-maximum effects, $[Zn^{2+}]_{0.5}$ in Table III. In order to compare the concentration dependences, corrections had to be introduced for chelation of Zn^{2+} by ATP, PP_i, and amino acids (see Appendix). The corrected values of $[Zn^{2+}]_{0.5}$ are presented in Table III. There are at least three classes of binding sites. The one with the highest affinity ($[Zn^{2+}]_{0.5}$ = 1–4 μM) is manifested as a decrease in the fluorescence intensity of the enzyme/TNS system and of the

Table IV: Dissociation Constants for Calculation of Free Zn^{2+}

chelator	pK_a	metal ion	$-\log K_{Me^+}$
Phe	9.18[a]	Zn^{2+}	4.50[b]
Gly	9.39[c]	Zn^{2+}	4.90[c]
ATP		Mg^{2+}	4.22[d]
		Zn^{2+}	4.85[d]

[a] Mooz (1976). [b] Perrin & Agarwal (1973). [c] Hallmann et al. (1971). [d] Khan & Martell (1966).

intrinsic tryptophan fluorescence, by stimulation of Ap_4A synthesis and by inhibition of adenylate synthesis and tRNA phenylalanylation. The second class (20–30 μM) corresponds to an increase in fluorescence intensity of the enzyme/TNS system, to inhibition of the stimulation of Ap_4A synthesis (Figure 1), and probably to additional inhibition of adenylate synthesis that is visualized indirectly via the steady-state concentration of the intermediate. The third class is revealed by protein aggregation.

Mechanism of Stimulation. Our data favor the idea that stimulation of Ap_4A synthesis is controlled by Zn^{2+}-induced conformational changes in the synthetase. It seems unlikely that stimulation is the result of chelation of Zn^{2+} with ATP. In this case, high concentrations of Mg^{2+} should have been inhibitory due to competition for ATP. This was, however, not observed (Plateau et al., 1981; Goerlich et al., 1982). It cannot be precluded that alternatively, Zn^{2+} is directly involved as a cofactor.

Of particular interest is the evidence that phenylalanine Zn^{2+} chelate might be involved in stimulation. The dependence of the concentration of phenylalanine was biphasic (Figure 2), suggesting, at first, nonequivalence of the active sites of the synthetase (Bartmann et al., 1975). However, analysis of the first partial reaction revealed that both active sites could synthesize phenylalanyladenylate equally well (Figure 4). The Michaelis–Menten constant at the high concentration portion of the curve in Figure 2 is 0.9 mM, in agreement with $K_{Zn^{2+},pH7.5}$ = 1.5 mM, the value of the dissociation constant of the phenylalanine Zn^{2+} chelate that was calculated according to eq 3 in the Appendix. The idea was corroborated by the finding that glycine, which was itself not a substrate, exhibited Zn^{2+}-dependent stimulation (Figure 2).

Protein Aggregation. Zn^{2+} caused reversible aggregation of phenylalanyl-tRNA synthetase. Whether this leads to further enzyme inactivation has not been determined. Such aggregation has been observed with many other proteins.

Half-maximal stimulation of Ap_4A synthesis was obtained at 3 μM free Zn^{2+} (12-fold rate acceleration; Table III). If a 3–4-fold acceleration is considered significant under in vivo conditions, levels of free Zn^{2+} must be at least 1 μM. Susceptibility of proteins to aggregation may occur at concentrations as low as 7–10 μM free Zn^{2+} or perhaps lower for particular proteins. If stimulation is important in vivo, protection against aggregation seems to be necessary.

Phenylalanyl-tRNA synthetase was protected by its substrates, whereas it was sensitized by Mg^{2+}. Phe (and Gly) and ATP also exerted nonspecific protection through chelation of Zn^{2+}. Consideration of in vivo effects, in particular of denaturation in the case of Zn^{2+}, should include the occurrence of protection by substrates.

Conclusion. Stimulation of Ap_4A synthesis by Zn^{2+} may be regarded as a side phenomenon of an enzyme in the process of being poisoned by a metal ion. Initially, the partial reaction that leads to Ap_4A and that is stimulated is rate limiting for the overall catalysis. As poisoning continues, the other partial reaction (adenylate synthesis) eventually takes over and stimulation ceases. At still higher concentrations of Zn^{2+} the enzyme begins to aggregate and eventually precipitates.

Zn^{2+} has been proposed as a regulatory factor in cell growth via its stimulatory effect on several aminoacyl-tRNA synthetases (Plateau et al., 1981; Goerlich et al., 1982), phenylalanyl-tRNA synthetase being among them. In addition to Zn^{2+}, levels of Mg^{2+} and ATP also control the rate of Ap_4A synthesis (Goerlich et al., 1982). Intracellular concentrations of Phe, insofar as they exceed those of phenylalanyl-tRNA synthetase, were not thought to contribute to the level of Ap_4A in the presence of unlimiting inorganic pyrophosphatase (Goerlich et al., 1982). Now that it has been shown that Phe promotes stimulation via its chelation of Zn^{2+}, its full range of intracellular concentrations could be effective.

All the considerations about regulation are based on the belief that cells could tolerate micromolar concentrations of free Zn^{2+}. We demonstrated that this level could be at the threshold for aggregation of proteins if they are not "stabilized" by their substrates or by other natural ligands. Intracellular compartmentation of stimulated aminoacyl-tRNA synthetases might also confer this "stability".

Acknowledgments

We gratefully acknowledge Dr. Kurt Ober, Regensburg, for the preparation of electron micrographs and Dr. Peter Orlean for reading and improving the manuscript.

Appendix

ATP, PP_i, phenylalanine, and glycine are known to form chelates with Zn^{2+} (Hallman et al., 1971; Perrin & Agarwal, 1973). Competition between Zn^{2+} and H^+ is taken into account for the amino acids at pH 7.5 by considering the respective dissociation constants

$$K_a = \frac{[A^-][H^+]}{[A] - [A^-]} \qquad A^- + H^+ \rightleftharpoons A^-H^+ \qquad (1)$$

$$K_{Zn^{2+}} = \frac{[A^-][Zn^{2+}]}{[A^-Zn^{2+}]} \qquad A^- + Zn^{2+} \rightleftharpoons A^-Zn^{2+} \qquad (2)$$

with [A], the concentration of Zn^{2+}-free amino acid. An apparent dissociation constant for complex A^-Zn^{2+} is calculated for any given pH according to

$$\frac{[A][Zn^{2+}]}{[A^-Zn^{2+}]} \equiv K_{Zn^{2+},pH} \equiv K_{Zn^{2+}}\frac{[H^+] + K_a}{K_a} \qquad (3)$$

Total concentrations in our experiments were such that $K_{Zn^{2+},pH} \gg [Zn^{2+}]_0 \ll [A]_0$, with $[A^-Zn^{2+}] = [Zn^{2+}]_0 - [Zn^{2+}]$. Values of $K_{Zn^{2+},pH}$ are calculated according to eq 3 from values in Table IV.

In the case of ATP and PP_i, Zn^{2+} competes with Mg^{2+}. Under our conditions, total concentrations follow the order

$$[Zn^{2+}]_0 \ll [ATP]_0 < [Mg^{2+}]_0 \qquad (4)$$

The ratio of concentrations of metal ion complexes with ATP is given by

$$\frac{[ATP{\cdot}Zn^{2+}]}{[ATP{\cdot}Mg^{2+}]} = \frac{K_{Mg^{2+}}}{K_{Zn^{2+}}}\frac{[Zn^{2+}]}{[Mg^{2+}]} \qquad (5)$$

with $K_{Zn^{2+}}$ and $K_{Mg^{2+}}$ the corresponding dissociation constants. Introduction of $[ATP{\cdot}Mg^{2+}] \simeq [ATP]_0$ into eq 5 and rearrangement gives

$$\frac{[ATP]_0[Zn^{2+}]}{[ATP{\cdot}Zn^{2+}]} = K_{Zn^{2+}}(app) = \frac{K_{Mg^{2+}}}{K_{Zn^{2+}}}([Mg^{2+}]_0 - [ATP]_0) \qquad (6)$$

The concentration of free Zn^{2+} in the presence of both Phe

and ATP was readily calculated if the ligands were in large excess, and concentration ratios r_{Phe} and r_{ATP} were computable from eq 3 and 6, respectively:

$$r_{Phe} = \frac{[Phe^{-}Zn^{2+}]}{[Zn^{2+}]} \qquad r_{ATP} = \frac{[ATP{\cdot}Zn^{2+}]}{[Zn^{2+}]} \tag{7}$$

Insertion into the approximate conservation equation

$$[Zn^{2+}]_0 - [Zn^{2+}] = [Phe^{-}Zn^{2+}] + [ATP{\cdot}Zn^{2+}] \tag{8}$$

gives

$$[Zn^{2+}] = [Zn^{2+}]_0 \frac{1}{1 + r_{Phe} + r_{ATP}} \tag{9}$$

Registry No. Ap_4A, 5542-28-9; TNS, 7724-15-4; Phe, 63-91-2; MgATP, 1476-84-2; Zn, 7440-66-6; phenylalanyl-tRNA synthetase, 9055-66-7; phenylalanyladenylate, 35874-27-2; lysyl-tRNA synthetase, 9031-26-9; pyruvate kinase, 9001-59-6; arginyl-tRNA synthetase, 37205-35-9; isoleucyl-tRNA synthetase, 9030-96-0; tryptophanyl-tRNA synthetase, 9023-44-3; tyrosyl-tRNA synthetase, 9023-45-4; aldolase, 9024-52-6; alcohol dehydrogenase, 9031-72-5; catalase, 9001-05-2; tryptophan synthase, 9014-52-2.

References

Baltzinger, M., & Holler, E. (1982) *Biochemistry 21*, 2460–2467, 2467–2476.

Bartmann, P., Hanke, T., & Holler, E. (1975) *Biochemistry 14*, 4777–4786.

Bernasconi, C. F. (1976) in *Relaxation Kinetics* (Bernasconi, C. F., Ed.) Academic Press, New York.

Berne, B. J. (1974) *J. Mol. Biol. 89*, 755–758.

Eagle, G. R., Zombola, R. R., & Himes, R. H. (1983) *Biochemistry 22*, 221–228.

Gaskin, F., Cantor, C. R., & Shelanski, M. L. (1974) *J. Mol. Biol. 89*, 737–755.

Goerlich, O., Foeckler, R., & Holler, E. (1982) *Eur. J. Biochem. 126*, 135–142.

Grummt, F. (1978) *Proc. Natl. Acad. Sci. U.S.A. 75*, 371–375.

Hallman, P. S., Perrin, D. D., & Watt, A. E. (1971) *Biochem. J. 121*, 549–555.

Hanke, T., Bartmann, P., Hennecke, H., Kosakowski, H. M., Jaenicke, R., Holler, E., & Böck, A. (1974) *Eur. J. Biochem. 43*, 601–607.

Kern, D., & Gangloff, J. (1981) *Biochemistry 20*, 2065–2075.

Kosakowski, H., & Holler, E. (1973) *Eur. J. Biochem. 38*, 274–282.

Mayaux, J.-F., & Blanquet, S. (1981) *Biochemistry 20*, 4647–4654.

Mooz, F. D. (1976) in *Handbook of Biochemistry and Molecular Biology* (Fasman, G. D., Ed.) 3rd ed., Vol. 1, pp 111–174, CRC Press, Cleveland, OH.

Perrin, D. D., & Agarwal, R. P. (1973) in *Metal Ions in Biological Systems* (Sigel, H., Ed.) Vol. 2, pp 167–206, Marcel Dekker, New York.

Pimmer, J., & Holler, E. (1979) *Biochemistry 18*, 3714–3723.

Plateau, P., Mayaux, J.-F., & Blanquet, S. (1981) *Biochemistry 20*, 4654–4662.

Rapaport, E., & Zamecnik, P. C. (1976) *Proc. Natl. Acad. Sci. U.S.A. 73*, 3984–3988.

Sillén, L. J., & Martell, A. E. (1964) in *Stability Constants of Metal-Ion Complexes*, The Chemical Society, London.

Zamecnik, P. C., Stephenson, M. L., Janeway, C. M., & Randerath, K. (1966) *Biochem. Biophys. Res. Commun. 24*, 91–97.

In Vitro Biosynthesis of Plasminogen in a Cell-Free System Directed by mRNA Fractions Isolated from Monkey Liver†

Mario Gonzalez-Gronow* and Kenneth C. Robbins

ABSTRACT: mRNA was isolated from total RNA of monkey liver by oligo(dT)–cellulose chromatography and was translated in a rabbit reticulocyte cell-free system. Analysis of the translation products immunoprecipitated with specific antibodies to monkey plasma plasminogen revealed a molecule with characteristics similar to those of native plasminogen. The purification of the mRNA by centrifugation on sucrose gradients indicated the presence of plasminogen mRNAs in both the 23S and 18S RNA fractions. Both plasminogen mRNAs can be further purified by chromatography on Sepharose 4B. Affinity chromatography of the proteins synthesized in vitro by total mRNA from liver, as well as by the purified mRNAs, on L-lysine-substituted Sepharose revealed that both major plasma plasminogen forms (1 and 2) are synthesized, as precursors, in the system. The in vitro synthesized plasminogen is similar in its physical and chemical properties to native plasma plasminogen as determined by its ability to bind to L-lysine-substituted Sepharose and its molecular interaction with streptokinase. The purified mRNAs were also translated in the presence of dog pancreas microsomal membranes, and the proteins sequestered inside the membranes were released and fractionated on concanavalin A–Sepharose. The 23S mRNA directed the synthesis of a plasminogen molecule similar to the circulating plasma plasminogen form 1, whereas the 18S mRNA directed the synthesis of a molecule similar to the circulating plasma plasminogen form 2. Our evidence indicates that the synthesis of the two major circulating plasma plasminogen forms is directed in the liver by separate mRNAs.

Plasminogen, the plasma zymogen of the fibrinolytic enzyme plasmin, is a single-chain protein with a molecular weight of about 88 000 containing 2% carbohydrate. It consists of 790 amino acids of known sequence (Sottrup-Jensen et al., 1978). Plasminogen is isolated from plasma by affinity chromatography on L-lysine-substituted Sepharose (Deutsch & Mertz, 1970) as two major forms (Brockway & Castellino, 1972) which differ in their states of glycosylation (Hayes & Castellino, 1979a–c). The active enzyme plasmin consists of two chains held together by disulfide bonds which are formed when the Arg_{560}–Val peptide bond of plasminogen is cleaved by a

† From the Division of Biochemistry, Michael Reese Research Foundation, Chicago, Illinois 60616. *Received May 23, 1983; revised manuscript received September 7, 1983.* This work was supported in part by U.S. Public Health Service Grant HL04366 from the National Heart, Lung and Blood Institute.

0006-2960/84/0423-0190$01.50/0